In-Situ Grafting of Hyperbranched Poly(ether ketone)s onto Multiwalled Carbon Nanotubes via the $A_3 + B_2$ Approach

Ja-Young Choi,[†] Se-Jin Oh,[†] Hwa-Jeong Lee,[†] David H. Wang,[‡] Loon-Seng Tan,[§] and Jong-Beom Baek*,[†]

School of Chemical Engineering, Chungbuk National University, Cheongju, Chungbuk 361-763, South Korea; University of Dayton Research Institute, 300 College Park Avenue, Dayton, Ohio 45469-0168; and Polymer Branch, Materials & Manufacturing Directorate, AFRL/MLBP, Air Force Research Laboratory, Wright-Patterson Air Force Base, Dayton, Ohio 45433-7750

Received January 17, 2007; Revised Manuscript Received April 7, 2007

ABSTRACT: Trimesic acid and phenyl ether were in-situ polymerized as A_3 and B_2 monomers, respectively, in the presence of a fixed amount (10 wt %) of multiwalled carbon nanotube (MWNT) to afford hyperbranched poly(ether ketone)s (PEK's)/MWNT nanocomposites. The feed ratios of A_3 and B_2 monomers vary from 3:2 to 1:2 in the $A_3 + B_2$ polycondensations. The polymerization was carried out in a mildly acidic medium, i.e., poly(phosphoric acid) or PPA, with an optimized amount of phosphorus pentoxide (P_2O_5) added. The overall evidence based on the data of elemental analysis (EA), thermogravimetric analysis (TGA), Fourier-transform infrared (FT-IR) spectroscopy, and scanning electron microscopy (SEM) implicates that hyperbranched PEK's were attached to the surface of MWNT to form hyperbranched PEK-*g*-MWNT nanocomposites. Furthermore, MWNT remained structurally intact under the polymerization and workup conditions. Evidently driven by the molecular architecture of globular hyperbranched polymers, the morphology of the nanocomposites resembles "mushroom-like clusters on MWNT stalks". The hyperbranched PEK-*g*-MWNT nanocomposites were soluble in polar aprotic solvents stemming from numerous carboxylic acids on their surfaces. When some of samples were dispersed in 1 M LiOH aqueous solutions, they formed very stable suspensions. The resulting lithiated nanocomposites are being investigated in the applications such as ion conductivity and energy capacitance.

Introduction

Carbon nanotubes (CNTs) such as single-walled carbon nanotubes (SWNTs), few-walled carbon nanotubes (FWNTs), and multiwalled carbon nanotubes (MWNTs) have generated great excitement in materials research because of the technological opportunities that their thermal, electrical, mechanical, and optical properties could offer. For example, they are being actively investigated for uses as reinforcing components to deliver outstanding properties to the polymeric matrices. The resulting nanocomposites would provide various potential applications, where affordable, lightweight, multifunctional materials are needed. In this view, MWNTs are more attractive from the standpoint of affordability when compared to SWNTs. Although their aspect ratios are lower than those of SWNTs, MWNTs are available in larger quantities, with higher purity (>97% carbon contents), and at reasonable prices. In general, MWNTs have diameters in the range of 10−20 nm and lengths on the order of 10−50 μm.[1,2] Their aspect ratios are still greater than 500, which are high enough to be used as reinforcement additives. However, there are two fundamental issues to be resolved in order to obtain maximal, enhanced properties using CNTs as nanoscale additives. One is to achieve the effective aspect ratio, which is largely dependent upon the state of dispersion.[3] The other one is to improve the interfacial adhesion between CNT surfaces and the matrix polymer.[4] Thus, many efforts have been made to attain homogeneous dispersion of CNTs in various matrix materials via physical methods aided by sonication,[5] chemical methods using strong acids,[6] or a combination of both.[7] However, structural damages to CNTs, which resulted from the treatment conditions such as power levels, exposure times, and temperatures, had occurred in many cases.[8] Even after homogeneous CNT dispersion has been achieved, the immediate issue is realizing strong interfacial adhesion between CNT and matrix. Thus, covalent bonding and/or strong noncovalent interactions between CNT and matrix are necessary to strengthen the CNT's reinforcement effect. Suitable chemical groups covalently attached to the surfaces of CNTs can hinder close lateral interactions among the nanotubes and also provide better chemical affinity to the matrix. The functionalized CNTs were dispersed in the matrices with higher degrees of exfoliation than the pristine ones.[9]

Recently, we have developed an effective Friedel−Crafts acylation reaction in optimized PPA/P_2O_5 medium[10] and

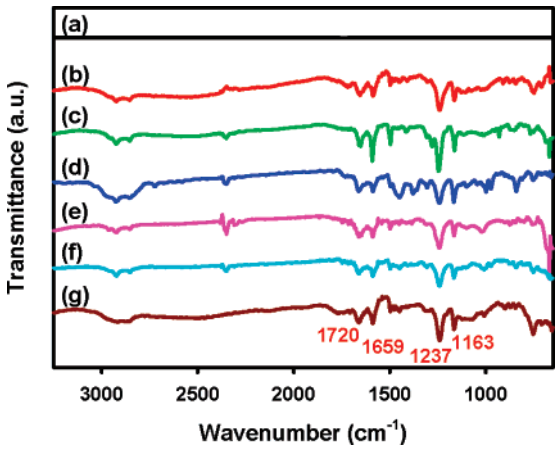

Figure 1. FT-IR spectra of (a) as-received MWNT, (b) **1a**, (c) **1b**, (d) **1c**, (e) **1d**, (f) **1e**, and (g) **1f**.

* Corresponding author: Tel +82-43-261-2489; Fax + 82-43-262-2380; e-mail jbbaek@chungbuk.ac.kr.
[†] Chungbuk National University.
[‡] University of Dayton Research Institute.
[§] Wright-Patterson Air Force Base.

10.1021/ma0701282 CCC: $37.00
Published on Web 05/25/2007

Scheme 1. Grafting of Hyperbranched PEK's onto MWNT from A_3 and B_2 Monomers

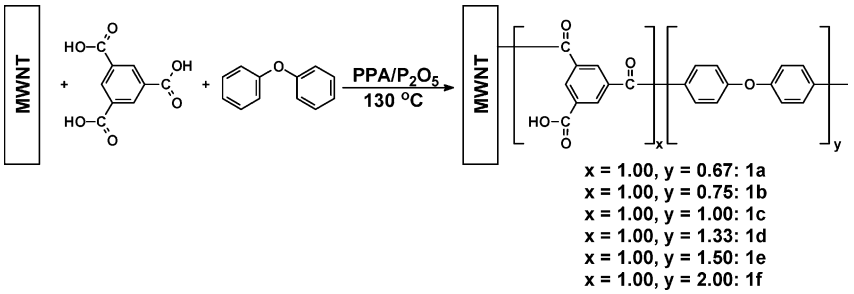

extended its application to chemical modifications of carbon nanomaterials such as carbon nanofibers (CNF) and MWNTs with organic moieties and linear poly(ether ketone)s (PEK's).[11] The reaction medium is moderately acidic but nondestructive to promote homogeneous dispersion of CNF and MWNTs and of relatively high viscosity to impede reaggregation of dispersed CNF and MWNTs. As a result, a uniform grafting onto CNF and MWNT has been shown to be achievable. We have also successfully grafted hyperbranched PEK's onto the surface of CNF using an AB_2 monomer via the same methodology.[12] Besides our work, to our knowledge, there are only very few examples in the literature that describe CNT or CNF covalently modified with dendritic polymers: (i) hyperbranched vinyl polymers grafted from MWNTs via atom transfer radical polymerization (ATRP);[13] (ii) hyperbranched poly(amidoamine)-modified MWNT via a "grafting-from" approach;[14] (iii) SWNTs grafted with poly(amidoamine) dendrimers using a divergent methodology.[15]

In this paper, we report that the reaction conditions that were developed and optimized for CNF modification are further applied to grafting hyperbranched PEK's onto the surface of MWNTs. In addition, as complementary to our previous work that entailed in-situ grafting a hyperbranched ether−ketone polymer to VGCNF using a suitable AB_2 monomer,[12] this work pertains to the grafting of a similar hyperbranched PEK to the surface of MWNTs using a newly discovered self-controlled polycondensation methodology directly from commercially available A_3 and B_2 monomers without the problem of gelation.[16]

Experimental Section

Materials. All reagents and solvents were purchased from Aldrich Chemical Inc. and used as received, unless otherwise mentioned. The monomer 1,3,5-benzenetricarboxylic acid (trimesic acid, mp >350 °C) was purified by recrystallization from water, and phenyl ether was purified by fractional distillation under reduced pressure. Multiwalled carbon nanotube (MWNT, CVD MWNT 95 with diameter 10−20 nm and length 10−50 μm) was obtained from Iljin Nanotech Co., LTD, Seoul, Korea.[17]

Instrumentation. Infrared (IR) spectra were recorded on Jasco FT-IR 480 Plus spectrophotometer. Solid samples were imbedded in KBr disks. Elemental analyses were performed by system support at CBNU with a CE Instruments EA1110. Differential scanning calorimetry (DSC) was performed under a nitrogen atmosphere with heating and cooling rates of 10 °C/min using a TA Instruments model MDSC2910 equipped with differential scanning calorimetry cell. The thermograms were obtained on powder samples after they had been heated to 300 °C and air-cooled to ambient temperature. Glass transition temperatures (T_g's) were generally taken as the midpoint of the baseline shift. Thermogravimetric analysis (TGA) was conducted in nitrogen and air atmospheres with a heating rate of 10 °C/min using a TA Instruments SDT 2960 thermogravimetric analyzer. The field emission scanning electron microscopy (FESEM) used in this work was LEO 1530FE.

Representative Procedure for in-Situ Grafting of Hyperbranched PEK's from A_3 and B_2 Monomers (2:3 Molar Ratio) with ~10 wt % MWNT Load. Into a 250 mL resin flask equipped with a high-torque mechanical stirrer and nitrogen inlet and outlet, trimesic acid (2.10 g, 10 mmol), phenyl ether (2.55 g, 15 mmol), MWNT (0.465 g), phosphorus pentoxide (P_2O_5, 15.0 g), and poly(phosphoric acid) (PPA, 60 g) were charged. The mixture was stirred at 100 °C for 12 h and heated to 130 °C. The mixture became homogeneous and stuck to the stirring rod, allowing no further efficient stirring at that temperature after 6 h. After the "cool down" period, water was added into the mixture and heated at 60−70 °C overnight under the nitrogen. The dark brown chunk was collected by suction filtration and washed with 5% hydrochloric acid and large amount of water. The product was further Soxhlet extracted with water for 2 days for the complete removal of PPA and methanol for 2 days for the removal of low molecular weight portions and finally dried under reduced pressure (0.05 mmHg) at 100 °C for 150 h to give 3.46 g (73% yield) of dark brown solid: Anal. Calcd for $C_{27}H_{16}O_6$: C, 76.36%; H, 3.69%. Found: C, 79.14%; H, 3.26%.

Results and Discussion

Grafting of Hyperbranched PEK's onto MWNT from A_3 and B_2 Monomers. One major concern on the synthesis of hyperbranched polymers via the $A_3 + B_2$ approach is the formation of cross-linked network. To avoid gelation as predicted in Carother's and Flory's statistical mechanics equations,[14] various attempts including dropwise addition of a diluted monomer solution[18] and the $A_2 + BB'_2$ approach[19] have been made to avoid gelation. We also developed a facile synthesis of hyperbranched PEK's via the $A_3 + B_2$ approach.[16] Because of the vast difference in the solubility of two monomers in the reaction medium, i.e., PPA, the gelation was prevented by a self-regulating manner. For example, the hydrophilic trimesic acid as an A_3 monomer was soluble in the hydrophilic reaction medium, while the hydrophobic phenyl ether (B_2 monomer) was only marginally soluble. The gelation was avoided for two reasons. One is automatic and slow feeding of the arylether monomer into the polymerization process due to its poor solubility. The other reason would be owing to the high viscosity of PPA/P_2O_5 medium containing trimesic acid (A_3 monomer), which effectively preclude hydrophilic growing molecules from having intimate contact with the B_2 comonomer (phenyl ether). Thus, hyperbranched polymers instead of cross-linked networks could be synthesized by such a self-regulating process.

In this manner, a series of hyperbranched ether−ketone polymers (**1a**−**f**) with different monomer (A_3:B_2) feed ratios was synthesized in the presence of MWNT in PPA/P_2O_5 medium at 130 °C to afford hyperbranched PEK-*g*-MWNT nanocomposites (Scheme 1).

All the polycondensations of trimesic acid and phenyl ether monomers were conducted at 130 °C in commercially available PPA (83% assay) with the additional 25 wt % of P_2O_5 and at ~5 wt % monomer concentrations according to the previously

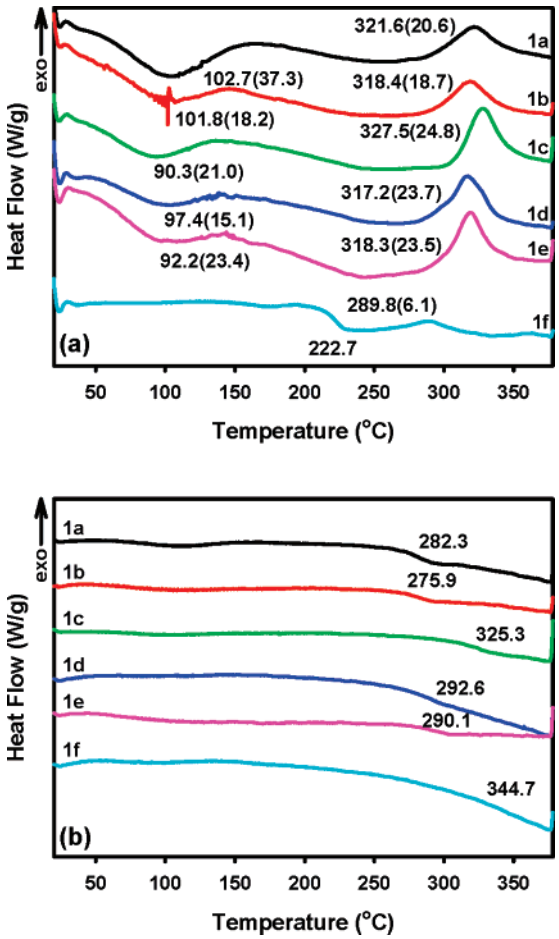

Figure 2. DSC thermograms of nanocomposites with heating rate of 10 °C/min: (a) first heating scan; (b) second heating scan.

Table 1. Monomer Feed Ratio, Yield and Elemental Analysis Data for MWNT-*g*-Hyperbranched PEK Nanocomposites

	monomer feed ratio[a]				elemental analysis		
sample	A_3	B_2	MWNT (wt %)	yield (%)		C (%)	H (%)
1a	1.00 (1.00)	0.67 (0.47)	10	48	calcd	71.81	3.16
					found	73.61	3.10
1b	1.00 (1.00)	0.75 (0.50)	10	73	calcd	72.60	3.22
					found	75.58	3.12
1c	1.00 (1.00)	1.00 (0.67)	10	73	calcd	74.15	3.40
					found	78.06	3.37
1d	1.00 (1.00)	1.33 (0.89)	10	76	calcd	75.71	3.58
					found	78.69	3.51
1e	1.00 (1.00)	1.50 (1.00)	10	73	calcd	76.52	3.64
					found	79.14	3.26
1f	1.00 (1.00)	2.00 (1.33)	10	85	calcd	78.11	3.80
					found	79.80	3.66

[a] The values in parentheses are the feed ratio of functional groups.

described procedure.[10] The reaction flask appeared initially dark black due to the heterogeneous dispersion of MWNT in the reaction mixture at 130 °C in 2 h. After that, the mixture became shinny black when MWNT was homogeneously dispersed. It appeared brownish-green when placed under a flash light, and the color change was probably due to the grafting of hyperbranched PEK's onto MWNT. In all cases, the mixture was homogeneous with drastic increase in the bulk viscosity at the end of the polymerization period. In fact, after only 6 h, the mixture was so viscous that an efficient stirring was practically impossible at 130 °C. After polymerization had been completed as judged visually by the bulk viscosity, distilled water was added into the polymerization mixture. The dark brown chunk

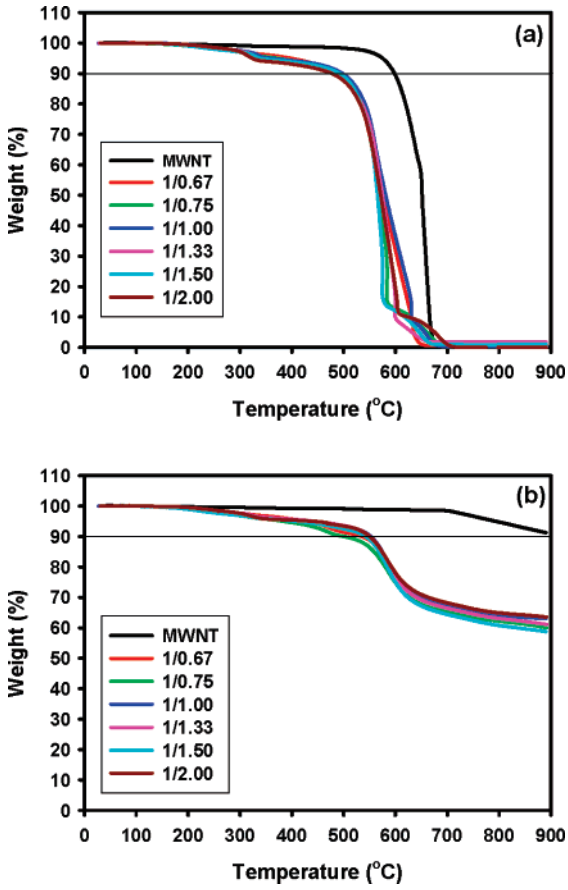

Figure 3. TGA thermograms of MWNT-*g*-hyperbranched nanocomposites with heating rate of 20 °C/min: (a) in air; (b) in nitrogen.

Table 2.. Thermal Properties of MWNT-*g*-Hyperbranched PEK Nanocomposite

	DSC[a]			TGA[b]			
				in air		in nitrogen	
sample	T_g (°C)	T_{exo} (°C)	ΔH_{exo} (J/g)	$T_{d10\%}$ (°C)	char at 900 °C (%)	$T_{d10\%}$ (°C)	char at 900 °C (%)
1a	282.3	321.6	20.6	485	0.54	530	63
1b	275.9	318.4	18.7	483	0.49	501	60
1c	325.3	327.5	24.8	498	0.35	552	63
1d	292.6	317.2	23.7	483	0.18	551	61
1e	290.1	318.3	23.5	492	1.08	543	59
1f	344.7	289.8	6.1	477	0.04	550	64

[a] Determined by DSC with heating rate of 10 °C/min. [b] The temperature at which 10% weight loss ($T_{d10\%}$) occurred on TGA thermogram obtained with heating rate of 10 °C/min.

of product was collected and washed with 5% hydrochloric acid and large amount of water. The product was subsequently Soxhlet-extracted with water for 2 days to ensure the complete removal of residual PPA and further extracted with methanol for 2 more days to remove any residual, unreacted monomers and low-molecular-weight homopolymer. Finally, it was dried under reduced pressure (0.05 mmHg) at 100 °C for 150 h to give 48−85% yield of a dark brown powder. We noted that the polymerization mixture of **1f** that was stuck to the stirring rod throughout the entire polymerization period appeared to be the most viscous among the series and also resulted in the highest isolation yield. In addition, we attribute the removal of the low-molecular-weight homopolymer portion to Soxhlet extraction; the experimental carbon contents determined by elemental analysis are higher than the theoretical values, which were calculated on the basis of 100% yield, while the hydrogen

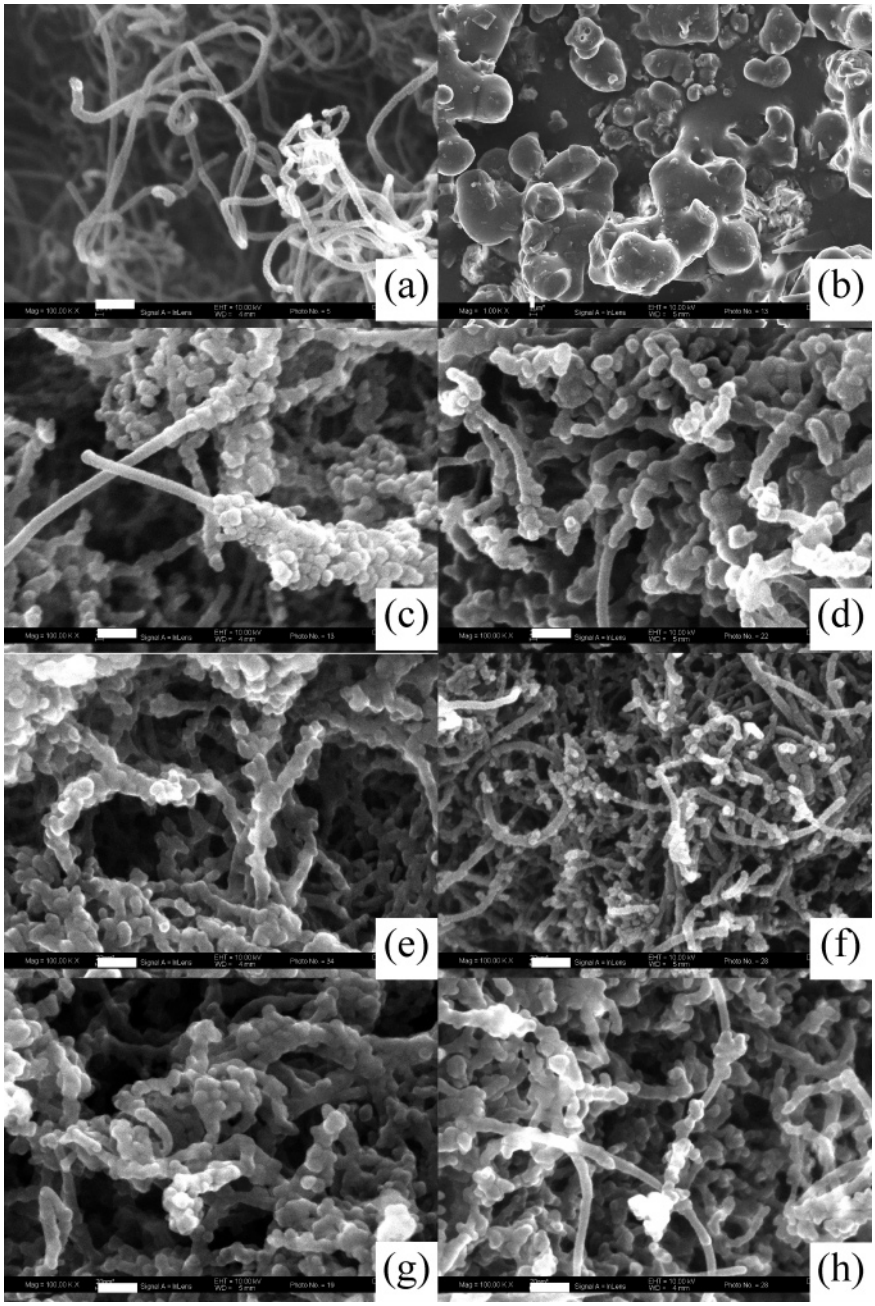

Figure 4. SEM images of (a) as-received MWNT (100 000×), (b) hyperbranched PEK homopolymer ($x = 1$; $y = 1.00$, 1000×), (c) **1a** (100 000×), (d) **1b** (100 000×), (e) **1c** (100 000×), (f) **1d** (100 000×), (g) **1e** (100 000×), and (h) **1f** (100 000×). Scale bars are 100 nm.

contents are slightly lower than the theoretical values (Table 1).

FT-IR Study. The FT-IR spectrum of as-received MWNTs exhibits weak sp^2 C−H and sp^3 C−H stretching bands, which were attributed to the defects at sidewalls and open ends of MWNTs.[20] These defects would provide sites for the electrophilic substitution reaction. In our previous work, FT-IR had been used to characterize the keto-carbonyl group covalently attached to the MWNT and vapor-grown carbon nanofiber (VGCNF) in PPA.[11] Therefore, this technique was used to verify the keto-carbonyl band at 1659 cm^{-1} associated with the Friedel−Crafts product and confirm the covalent attachment of hyperbranched PEK's to MWNT (Figure 1). There was also a strong carboxylic-carbonyl band at 1720 cm^{-1}, stemming from the large numbers of carboxylic acids at the ends of hyperbranched PEK's. Soxhlet extraction of MWNT-*g*-hyperbranched PEK's with hot methanol, which is a fairly good solvent for the carboxylic acid-terminated hyperbranched PEK homopolymers, was carried out to extract the unattached, low-molar-mass homopolymer. On the basis of the FT-IR results of Soxhlet-treated nanocomposites and our previous model compound study, [11a] we are certain that hyperbranched polymers have been successfully attached onto MWNT covalently. However, because of experimental difficulty, the degree of branching (linear defect) was not determined.

Solution Properties. The solubility of the nanocomposites varied according to the monomer feed ratios due to the polarity of the surface groups and the PEK's molecular weights. For example, as B_2 aryl ether monomer feed value was decreased from 2.0 to 0.67 (see Table 1), the average degree of polymerization would decrease and the number of carboxylic acids would increase accordingly. Thus, the nanocomposites became more hydrophilic with less B_2 monomer feed. The solubility of nanocomposites in polar aprotic solvents such as *N*,*N*-dimeth-

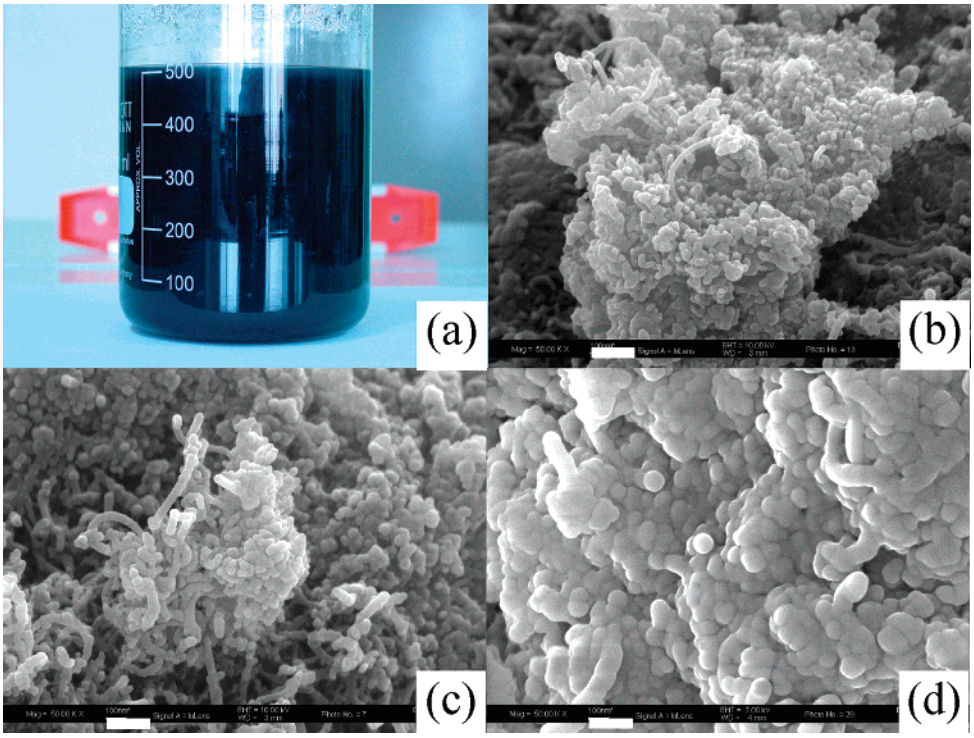

Figure 5. (a) Digital photograph of lithiated **1b**. (b) SEM image of lithiated **1b** (50 000×). (c) SEM image of lithiated **1e** (50 000×). (d) SEM image of lithiated **1f** (50 000×). Scale bars are 200 nm.

ylformamide (DMF), *N*,*N*-dimethylacetamide (DMAc), dimethyl sulfoxide (DMSO), and *N*-methyl-2-pyrrolidinone (NMP) was higher than 1 wt % (10 g/kg), and there were almost no insoluble gels observed. Furthermore, substantial portions of nanocomposites, presumably samples with low-molecular-weight grafts, were soluble even in acetone.

Thermal Properties. The DSC samples (powder form) were subjected to two cycles of heating from room temperature to 380 °C and then cooling to room temperature with the same heating and cooling rate of 10 °C/min (Figure 2). Because of the hygroscopic nature of the nanocomposite samples, which contained a large number of carboxylic acid termini, broad endothermic peaks were detected in the range 90−103 °C resulting from the evaporation of residual water (Figure 2a). For all nanocomposite samples, we also observed the thermal relaxation of viscosity- and shear-induced strain, a thermal phenomenon driven by the high-viscosity nature of the reaction medium, PPA/P_2O_5, that was previously reported by us.[21] The exotherms of as-isolated (i.e., before heat treatment) samples were attributed to the kinetically stored strain energy (∼6−25 J/g) induced by the shear field (generated by mechanically stirring and spreading the polymerization mixture against the walls of the reaction vessel) during polymerization reaction at 130 °C. During the cooling down period after the polymerization, the viscosity of poly(phosphoric acid) must have increased much faster than the relaxation process of the strained polymer structures, leading to the storage of such strain energy upon aqueous workup of the polymerization mixture. When the as-isolated samples were heated to the temperatures close to T_g, the "frozen" polymer chains started to move, releasing the strain energy. Interestingly, exothermic peak for sample **1c** is the narrowest and has the highest ΔH_{exo} value, indicating that the molecular motion is the most constrained (Figure 2a). The glass-transition temperature (T_g) value was taken as the midpoint of the maximum baseline shift from each run. The T_g's of the nanocomposites are in the range of 276 and 325 °C (Figure 2b and Table 2). For the samples **1c**, it was ∼63 °C higher than the pure hyperbranched PEK, which was prepared using the same monomer stoichiometry and whose T_g was 262 °C.[19a] This relatively large increase in T_g is probably due to the restriction of the molecular motion after the polymer chains have been attached to MWNT, and perhaps, enhanced intermolecular hydrogen bonding among the carboxylic groups.

The thermogravimetric analysis (TGA) experiments on the powder samples from **1a** to **1f** displayed that the temperatures at which a 10% weight loss ($T_{d10\%}$) in air occurred at 485, 483, 498, 483, 492, and 477 °C in that order (Figure 3a) and in nitrogen at 530, 501, 552, 551, 543, and 550 °C in that order (Figure 3b). The weight losses of all samples occurred around 300 °C for both in air and in nitrogen are ascribed to the early degradation of carboxylic acids (decarboxylation). Because of large amounts of chain-end carboxylic acids associated with the hyperbranched PEK, all the nanocomposites lost about 5 wt % around 350 °C in both air and nitrogen. The functionalized VGCNF exhibited two-stage degradation in air, which was used to calculate the VGCNF contents.[11] However, some hyperbranched PEK-*g*-MWNT nanocomposites did not show a clear-cut, two-stage degradation, and some only displayed one-stage degradation in air, which made it difficult to determine the MWNT contents (Figure 3a).

Scanning Electron Microscopy (SEM). The SEM image of pristine MWNT shows that the tube surfaces are seamless and smooth (Figure 4a). A large amount of hyperbranched polymer attached to MWNT can be observed from the images of **1a**−**1f** (Figure 5c−h). Molecular architecture of 3-dimensional dendritic macromolecules such as dendrimers and hyperbranched polymers are known to be globular (Figure 4b). Thus, the images look like "mushroom-like clusters on MWNT stalks". As the B_2 monomer feed ratio decreased, the surface nature of nanocomposites would become more polar to form smooth surface due to the possibility of stronger intramolecular hydrogen bonding (from Figure 4c to 4f). Interestingly, sample **4d** has the thickest average diameter among the nanocomposites. This may be due to the strongest lateral interaction along the tube

direction, and thus some tubes aggregate to form bundles, each comprising several tubes. Coincidently, the average diameter of the sample **4d** is ~70 nm, which is 3 times thicker than that of unmodified MWNT (diameter of ~10−20 nm). Similar results have been obtained for the functionalized MWNT's with various surface functionalities.[22] In this study, MWNTs containing polar surface groups such as amino, hydroxyl, and fluorine groups displayed similar an assembling tendency to form tetragonal or hexagonal packing depending upon the strength of surface polarity while MWNTs functionalized with less polar groups such as methoxy, ethoxy, bromine, and chlorine groups appeared to be mostly individual tubes. Thus, hyperbranched PEK-*g*-MWNTs could possibly form hexagonal packing as expected due to the high polarity on their surfaces. Particularly, the hyperbranched polymer, which has more polar carboxylic acids as termini, is more likely to display such a lateral assembly.

Because of numerous surface carboxylic acid groups that are able to ionize in basic environment, MWNT-*g*-hyperbranched PEK **1b** was readily dispersed in LiOH solution (1 M) in water-forming stable suspension (Figure 5a). It was still homogeneous after a month of standing under room conditions. A portion of suspension was taken out and allowed to slowly evaporate off the water. The resulting specimen was examined by SEM. In comparing the SEM image to that of **1b** (Figure 4d), one can see that the lithiated hyperbranched PEK-*g*-MWNT **1b** shows heavy amounts of lithium ions uniformly decorated on the surface of the nanocomposite (Figure 5b). Similar morphology was obtained from lithiated **1e** (Figure 5c). For example, the diameter of MWNT still maintained ~40 nm and the tube surfaces of the lithiated **1e** were as rough as before the lithiation as shown in Figure 4g. However, lithiated sample **1f** has a much thicker diameter of ~100 nm and the surfaces are relatively uniform (Figure 5d). A study on their electrochemical properties is currently underway.

Conclusion

The results presented in this study suggest that the MWNT nanocomposites via an in-situ $A_3 + B_2$ polymerization are a viable and practical approach to grafting hyperbranched ether−ketone polymers onto MWNT, using commercially available raw materials. The self-regulating facet that relies on the vast difference in the solubility of A_3 and B_2 monomers in the polymerization medium is undoubtedly the key to the success of this approach. Another important advantage of this methodology is that by simply varying the A_3:B_2 monomer feed ratio it is possible to alter the polarity of the resulting nanocomposites, changing from highly ionizable (theoretically 100% CO_2H end groups when A_3:B_2 = 1:1) to relatively nonpolar (theoretically 100% phenoxy end groups when A_3:B_2 = 1:2). Because of the globular molecular architecture of hyperbranched polymers, the morphology of the nanocomposites could be vividly described as "mushrooms on the MWNT stalks". The resultant organo-soluble/dispersible nanocomposites could be used as structural additives to the polymer matrices. In addition, we have found that the lithiated nanocomposites from lithium ion-proton exchange did form stable suspensions in water, and the studies of their electrochemical behaviors such as ion conductivity and energy capacitance are presently in progress.

Acknowledgment. We are grateful to Jeong Hee Lee of Chungbuk National University for conducting SEM. This project was supported by funding from the research grant of Chungbuk National University in 2005.

References and Notes

(1) Carneiro, O. S.; Covas, J. A.; Bernardo, C. A.; Caldeira, G.; Hattum, F. W. J. V.; Ting, J. M.; Alig, R. L.; Lake, M. L. *Compos. Sci. Technol.* **1998**, *58*, 401−407.

(2) Singh, C.; Quested, T.; Boothroyd, C. B.; Thomas, P.; Kinloch, I. A.; Abou-Kandil, A. I.; Windle, A. H. *J. Phys. Chem. B* **2002**, *106*, 10915−10922.

(3) Song, Y. S.; Youn, J. R. *Carbon* **2005**, *43*, 1378.

(4) (a) Ajayan, P. M.; Schadler, L. S.; Giannaris, C.; Rubio, A. *Adv. Mater.* **2000**, *12*, 750. (b) Calvert, P. *Nature (London)* **1999**, *399*, 210. (c) Lourie, O.; Wagner, H. D. *J. Mater. Res.* **1998**, *13*, 2418. (d) Cadek, M.; Coleman, J. N.; Ryan, K. P.; Nicolosi, V.; Bister, G.; Fonseca, A.; Nagy, J. B.; Szostak, K.; Béguin, F.; Blau, W. J. *Nano Lett.* **2004**, *4*, 353.

(5) (a) Zhang, W. D.; Shen, L.; Phang, I. Y.; Liu, T. *Macromolecules* **2004**, *37*, 256. (b) Liu, T.; Phang, I. Y.; Shen, L.; Chow, S. Y.; Zhang, W. D. *Macromolecules* **2004**, *37*, 7214. (c) Andrews, R.; Jacques, D.; Rao, A. M.; Rantell, T.; Derbyshire, F.; Chen, Y.; Chen, J.; Haddon, R. C. *Appl. Phys. Lett.* **1999**, *75*, 1329. (d) Qian, D.; Dickey, E. C.; Andrews, R.; Rantell, T. *Appl. Phys. Lett.* **2000**, *76*, 2868. (e) Shaffer, M. S. P.; Windle, A. H. *Adv. Mater.* **1999**, *11*, 937. (f) Zin, L.; Bower, C.; Zhou, O. *Appl. Phys. Lett.* **1998**, *73*, 1197. (g) Haggenmueller, R.; Gommans, H. H.; Rinzler, A. G.; Fischer, J. E.; Winey, K. I. *Chem. Phys. Lett.* **2000**, *330*, 219. (h) Chen, G. Z.; Shaffer, M. S. P.; Coleby, D.; Dixon, G.; Zhou, W.; Fray, D. J.; Windle, A. H. *Adv. Mater.* **2000**, *12*, 522. (i) Dupire, M.; Michel, J. European Patent 1,054,036A1, Nov 22, 2000. (j) Sandler, J.; Shaffer, M. S. P.; Prasse, T.; Bauhofer, W.; Schulte, K.; Windle, A. H. *Polymer.* **1999**, *40*, 5967. (k) Part, C.; Ounaies, Z.; Watson, K. A.; Crooks, R. E.; Smith, Jr., J.; Lowther, S. E.; Connell, J. W.; Siochi, E. J.; Harrison, J. S.; St. Clair, T. L. *Chem. Phys. Lett.* **2002**, *364*, 303.

(6) (a). Sun, Y.-P.; Fu, K.; Lin, Y.; Huang, W. *Acc. Chem. Res.* **2002**, *35*, 1096. (b) Dai, L.; Mau, W. H. *Adv. Mater.* **2001**, *13*, 899. (c) Hirsch, A. *Angew. Chem., Int. Ed.* **2002**, *41*, 1853. (d) Banerjee, S.; Kahn, M. G. C.; Wong, S. S. *Chem.—Eur. J.* **2003**, *9*, 1898. (e) Tasis, D.; Tagmatarchis, N.; Georgakilas, V.; Prato, M. *Chem.—Eur. J.* **2003**, *9*, 4000. (e) Lin, Y.; Zhou, B.; Shiral Fernando, K. A.; Liu, P.; Allard, L. F.; Sun, Y.-P. *Macromolecules* **2003**, *36*, 7199. (f) Mitchell, C. A.; Bahr, J. L.; Arepalli, S.; Tour, J. M.; Krishnamoorti, R. *Macromolecules* **2002**, *35*, 8825.

(7) (a) Huang, W.; Lin, Y.; Taylor, S.; Gaillard, J.; Rao, A. M.; Sun, Y.-P. *Nano Lett.* **2002**, *2*, 231. (b) Sandler, J.; Shaffer, M. S. P.; Prasse, T.; Bauhofer, W.; Schulte, K.; Windle, A. H. *Polymer.* **1999**, *40*, 5967. (c) Kumar, S.; Dang, T. D.; Arnold, F. E.; Bhattacharyya, A. R.; Min, B. G.; Zhang, X.; Vaia, R. V.; Park, C.; Wade, W. W.; Hauge, R. H.; Smalley, R. E.; Ramesh, S.; Willis, P. A. *Macromolecules* **2002**, *35*, 9039.

(8) Heller, D. A.; Barone, P. W.; Strano, M. S. *Carbon* **2005**, *43*, 651.

(9) (a) Shaffer, M. S. P.; Fan, X.; Windle, A. H. *Carbon* **1998**, *36*, 1603. (b) Cai, L.; Bahr, J. L.; Yao, Y.; Tour, J. M. *Chem. Mater.* **2002**, *14*, 4235. (c) Mickelson, E. T.; Huffman, C. B.; Rinzler, A. G.; Smalley, R. E.; Hauge, R. H.; Margrave, J. L. *Chem. Phys. Lett.* **1998**, *296*, 188. (d) Bahr, J. L.; Yang, J.; Kosynkin, D. V.; Bronikowski, M. J.; Smalley, R. E.; Tour, J. M. *J. Am. Chem. Soc.* **2001**, *123*, 6536. (e) Bahr, J. L.; Tour, J. M. *Chem. Mater.* **2001**, *13*, 3823. (f) Mitchell, C. A.; Bahr, J. L.; Arepalli, S.; Tour, J. M.; Krishnamoorti, R. *Macromolecules* **2002**, *35*, 8825.

(10) Baek, J.-B.; Tan, L.-S. *Polymer* **2003**, *44*, 4135.

(11) (a) Baek, J.-B.; Lyons, C. B.; Tan, L.-S. *J. Mater. Chem.* **2004**, *14*, 2052. (b) Baek, J.-B.; Lyons, C. B.; Tan, L.-S. *Macromolecules* **2004**, *37*, 8278. (c) Oh, S.-J.; Lee, H.-J.; Keum, D.-K.; Lee, S.-W.; Wang, D. H.; Park, S.-Y.; Tan, L.-S.; Baek, J.-B. *Polymer* **2006**, *47*, 1132−1140.

(12) Wang, D. H.; Baek, J.-B.; Tan, L.-S. *Mater. Sci. Eng., B* **2006**, *132*, 103.

(13) Hong, C.-Y.; You, Y.-Z.; Wu, D.; Liu, Y.; Pan, C.-Y. *Macromolecules* **2005**, *38*, 2606.

(14) Cao, L.; Yang, W.; Yang, J.; Wang, C.; Fu, S. *Chem. Lett.* **2004**, *33*, 490.

(15) Campidelli, S.; Sooambar, C.; Diz, E. L.; Ehli, C.; Guldi, D. M.; Prato, M. *J. Am. Chem. Soc.* **2006**, *128*, 12544.

(16) (a) Choi, J.-Y.; Baek, J.-B.; Tan, L.-S. *Macromolecules* **2006**, *39*, 9057. (b) Baek, J.-B.; Lyons, C. B.; Tan, L.-S. *Polym. Prepr. (Am. Chem. Soc., Div. Polym. Chem.*) **2004**, *45*, 647−648.

(17) http://www.iljinnanotech.co.kr.

(18) (a) Fang, J.; Kita, H.; Okamoto, K. *Macromolecules* **2000**, *33*, 6937. (b) Fang, J.; Kita, H.; Okamoto, K. *J. Membr. Sci.* **2001**, *182*, 245. (c) Czupik, M.; Fossum, E. *J. Polym. Sci., Part A: Polym. Chem.* **2003**, *41*, 3871. (d) Bharathi, P.; Moore, J. S. *Macromolecules* **2000**, *33*,

3212. (e) Bernal, D. P.; Bedrossian, L.; Collins, K.; Fossum, E. *Macromolecules* **2003**, *36*, 333. (f) Lin, Q.; Long, T. L. *Macromolecules* **2003**, *36*, 9809.
(19) (a) Chang, Y.-T.; Shu, C.-F. *Macromolecules* **2003**, *36*, 661. (b) Liu, Y.; Chung, T.-S. *J. Polym. Sci., Part A: Polym. Chem.* **2002**, *40*, 4563.
(20) Lee, H.-J.; Oh, S.-J.; Choi, J.-Y.; Kim, J. W.; Han, J.; Tan, L.-S.; Baek, J.-B. *Chem. Mater.* **2005**, *17*, 5057−5064.
(21) Baek, J.-B.; Park, S. Y.; Price, G. E.; Lyons, C. B.; Tan, L. S. *Polymer* **2004**, *46*, 1543.
(22) Lee, H.-J.; Oh, S.-J.; Keum, D.-K.; Tan, L.-S.; Baek, J.-B. *Polym. Prepr. (Am. Chem. Soc., Div. Polym. Chem.)* **2005**, *46*, 216.

MA0701282